2019

Effect of Fabric Deformation on Thermal Protective Performance of Clothing in a Cylindrical Configuration

Yun Su
Donghua University

Rui Li
Iowa State University, ruili@iastate.edu

Jie Yang
Xi'an University

Guowen Song
Iowa State University, gwsong@iastate.edu

Chunhui Xiang
Iowa State University, chxiang@iastate.edu

See next page for additional authors

Effect of Fabric Deformation on Thermal Protective Performance of Clothing in a Cylindrical Configuration

Abstract

Firefighting protective clothing is designed to provide thermal protection for firefighters in fire extinguishing or rescuing operations. However, fabric deformation and stretching due to body movement and different postures could change the clothing's thermal protective performance. Current gaps in our knowledge with regard to fabric deformation often resulted in biased predictions of the thermal protective level that personal protective equipment (PPE) can provide, highlighting the need to improve our understanding in this field. In this study, we developed a device that can be connected to a cylindrical copper calorimeter to simulate fabric deformation due to body movement and different postures and simultaneously measure the fabric's thermal properties. Stretching forces of varying magnitudes (of 0, 1.2, 2.1, and 3.1 psi) were applied to study the effect of fabric deformation on the thermal protective performance of clothing under low- and high-intensity heat exposures. In addition, we analyzed skin burn times with different stretching forces and fabric properties. The selected fabrics were stretched by approximately 15 % under a stretching force of 3.1 psi. Fabric deformation led to a significant reduction of the predicted thermal protective performance of fabrics, mainly due to changes in fabric thickness, porosity, and mass per unit area. Predicted skin burn times decreased for increasing stretching forces, although the decrease was less pronounced under high-intensity heat exposure as a result of fabric shrinkage and degradation. The findings from this study further advance our current understanding of the thermal protective performance of clothing and may lead to the development of a new test to characterize clothing performance under more realistic usage situations.

Keywords

fabric deformation, thermal protective performance, clothing, body movement, stretching force

Disciplines

Fiber, Textile, and Weaving Arts | Industrial and Product Design | Performance Studies | Psychology of Movement

Comments

This book chapter is published as Y. Su, R. Li, J. Yang, G. Song, C. Xiang, and J. Li, “Effect of Fabric Deformation on Thermal Protective Performance of Clothing in a Cylindrical Configuration,” in Homeland Security andPublic Safety: Research, Applications, and Standards, ed. P. J. Mattson and J. L. Marshall (West Conshohocken, PA: ASTM International, 2019), 271–285. Doi: 10.1520/ STP1614201800595

Authors

Yun Su, Rui Li, Jie Yang, Guowen Song, Chunhui Xiang, and Jun Li

STP 1614, 2019 / available online at www.astm.org / doi: 10.1520/STP161420180059

Yun Su,[1,2] Rui Li,[3] Jie Yang,[4] Guowen Song,[3] Chunhui Xiang,[3] and Jun Li[1,2]

Effect of Fabric Deformation on Thermal Protective Performance of Clothing in a Cylindrical Configuration

Citation

Y. Su, R. Li, J. Yang, G. Song, C. Xiang, and J. Li, "Effect of Fabric Deformation on Thermal Protective Performance of Clothing in a Cylindrical Configuration," in *Homeland Security andPublic Safety: Research, Applications, and Standards*, ed. P. J. Mattson and J. L. Marshall (West Conshohocken, PA: ASTM International, 2019), 271–285. http://doi.org/10.1520/STP161420180059[5]

ABSTRACT

Firefighting protective clothing is designed to provide thermal protection for firefighters in fire extinguishing or rescuing operations. However, fabric deformation and stretching due to body movement and different postures could change the clothing's thermal protective performance. Current gaps in our knowledge with regard to fabric deformation often resulted in biased predictions of the thermal protective level that personal protective equipment (PPE) can provide, highlighting the need to improve our understanding in this field. In this study, we developed a device that can be connected to a cylindrical copper calorimeter to simulate fabric deformation due to body movement and different postures and simultaneously measure the fabric's thermal properties. Stretching forces of varying magnitudes (of 0, 1.2, 2.1, and 3.1 psi) were applied to study the

Manuscript received August 21, 2018; accepted for publication April 5, 2019.

[1]College of Fashion and Design, Donghua University, No. 1882, West Yan-An Rd., Shanghai 200051, China
Y. S. https://orcid.org/0000-0001-8697-4284

[2]Key Laboratory of Clothing Design and Technology, Donghua University, Ministry of Education, China No. 1882, West Yan-An Rd., Shanghai 200051, China

[3]Iowa State University, 515 Morrill Rd., Ames, IA 50010, USA

[4]College of Safety Science and Engineering, Xi'an University of Science and Technology, No. 58, Yan-ta Middle Rd., Beilin District, Xi'an 710054, China

[5]ASTM Symposium on *Homeland Security and Public Safety: Research, Applications, and Standards* on June 28–29, 2018 in San Diego, CA, USA.

effect of fabric deformation on the thermal protective performance of clothing under low- and high-intensity heat exposures. In addition, we analyzed skin burn times with different stretching forces and fabric properties. The selected fabrics were stretched by approximately 15 % under a stretching force of 3.1 psi. Fabric deformation led to a significant reduction of the predicted thermal protective performance of fabrics, mainly due to changes in fabric thickness, porosity, and mass per unit area. Predicted skin burn times decreased for increasing stretching forces, although the decrease was less pronounced under high-intensity heat exposure as a result of fabric shrinkage and degradation. The findings from this study further advance our current understanding of the thermal protective performance of clothing and may lead to the development of a new test to characterize clothing performance under more realistic usage situations.

Keywords

fabric deformation, thermal protective performance, clothing, body movement, stretching force

Introduction

Firefighting protective clothing has been widely used to shield firefighters from injury in a wide range of firefighting situations.[1] The protective clothing is capable of resisting fire and heat transfer, thus providing firefighters with additional time to extinguish fires and perform emergency rescue operations. Thermal protective performance provided by the clothing directly determines the safety and health of firefighters in fire hazards.

Recent decades have seen an increasing amount of research into the thermal protective performance of clothing. Typically, these studies are carried out in three different heat scenarios: low-, medium-, and high-intensity heat exposure representing routine, hazardous, and emergency fire scenarios, respectively. A test device using stored thermal energy[2] is employed to evaluate the thermal protection under low-level thermal radiation, while thermal protective performance (TPP)[3] and radiative protective performance (RPP)[4] testers are used to simulate medium-to high-intensity heat exposure. In these tests, the Stoll criteria was used to estimate the time to skin burn, which in turn serves as a criterion to evaluate a fabric's TPP. Since the Stoll criteria combine cumulative thermal energy with tolerance time to second-degree skin burn under constant heat exposure,[5] they are not used to predict third-degree skin burn.[6] Pennes' bio-heat transfer model[7] can be coupled with Henriques' burn model[8] to evaluate second- and third-degree skin burn injuries under transient heat exposures, resulting in a tool with a wide variety of practical applications for assessing TPP.

Using standardized test approaches, several studies identified the key factors affecting TPP. They consist of basic fabric properties such as thickness, density, component, thermal conductivity, and specific heat,[9–11] as well as clothing style.[12,13] The volume and distribution of air pockets separating the clothing from the human

body also has an important impact on thermal protective properties.[14,15] While moisture in protective clothing could enhance its protective capabilities (positive effect), it could also cause skin scalding or steam burns due to the penetration of water vapor molecules into the skin (negative effect).[16,17] The positive or negative effect depends on moisture content and distribution, exposure intensity and time, and fabric properties.[16,17]

In real firefighting scenarios, firefighters are constantly moving, which changes the amount and volume of air gaps caught under the fabric. Xin, Li, and Li[18] developed an improved TPP tester to examine the effect of constantly changing air gaps on the clothing's thermal protective performance under 84 kW/m^2 convective/radiative heat exposure. Ghazy and Bergstrom[19] developed a numerical model for dynamic air gaps smaller than 6.4 mm to investigate the effect of air gap size frequency and amplitude variations on the clothing's protective properties. This dynamic air gap model was further improved by using computational fluid dynamics (CFD) to simulate the effect of body movement on air gap size and orientation.[20] Physical movement by the wearer not only changes the air gap size but can also result in fabric deformation.[21] It has been reported that fabric deformation can change a fabric's basic properties, such as thickness, density, and air permeability. In a previous study, Li et al.[21] developed a fixed-length tensile device to study the effect of fabric deformation on the TPP. However, this test device was of a planar configuration that cannot account for body geometry or simulate fabric compression due to a stretching force. A cylindrical configuration is better suited as it can account for the curved surface of a human body and for the effects of body movement and different postures on fabric properties. Furthermore, there is a significant difference in fabric shrinkage between planar and cylindrical configurations.[22]

Therefore, the main objective of this study was to investigate the effect of fabric deformation, caused by body movement, on the TPP of clothing using a cylindrical configuration. To address this question, we developed a stretching device that connects to a cylindrical copper calorimeter and combined it with a traditional TPP test device where we replaced the planar copper calorimeter. Four kinds of stretching forces were applied in low- and high-intensity heat exposures to evaluate the TPP of clothing. We then measured changes in the fabric's basic properties and its TPP for different stretching forces. The findings from this study will contribute to the development of new and more realistic approaches for evaluating the TPP of clothing subjected to movement-related stretching forces.

Experimental

MATERIALS

Typically, firefighting protective clothing consists of three different fabric layers (i.e., an outer shell, a moisture barrier, and a thermal liner). Since the outer shell—providing a higher flame-retardant property, strength, and heat stability—is

extremely important for the clothing system, we only tested the shell fabric in this study,[23] in particular, three different types of flame-resistant fabrics commonly used to produce shell fabrics. Based on the size of our cylindrical sensor assembly, the fabric sample was cut into rectangular pieces of dimensions 115 mm by 450 mm, with the cuts performed along the 45° direction of fabric warp in order to be able to easily mimic fabric deformation.[21] Prior to the test, all specimens were conditioned in a standard atmosphere (20°C and 65 % relative humidity) for at least 24 hours.

INSTRUMENT DESIGN AND CONFIGURATION

Due to the nature of their work, firefighters perform many physical activities and assume several different postures when extinguishing fires and performing rescue operations. These include: walking, running, crouching, crawling, and climbing ladders. As a result, firefighting protective clothing can undergo complex deformations especially near the joints (knees, elbows, and shoulders). Figure 1 illustrates the change of air gap size and fabric deformation around a knee, due to body movement or when assuming different postures. Movement changes the air gap size and causes the fabric to stretch along the vertical direction.

In order to simulate the effect of body movement on air gap size and fabric deformation, we developed a new stretching device that is connected to a cylindrical sensor assembly. This device is composed of a specimen fixing component, an air cylinder, an air gap simulator, and a cylindrical copper calorimeter. The specimen is fixed by four lock pins and two spring clips. The stretching forces can be applied to the specimen by raising one of the fixed components using compressed air. The rise of the compressor stretches the fabric system. By controlling the output

FIG. 1 Change of air gap size and fabric deformation around a human leg for different movements and postures.[24]

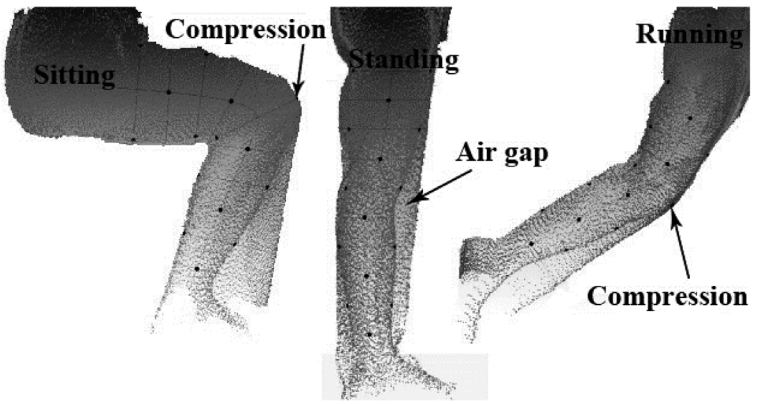

pressure of the air cylinder, we can apply tensile pressures that range from 1.2 to 3.1 psi. The air gap simulator has a thickness of 6.4 mm, which is sufficient to simulate a realistic microclimate between the clothing and the human body.[2] The test specimen can be brought in direct contact with the cylindrical copper calorimeter by removing the air gap simulator. The cylindrical copper calorimeter consists of a 25 mm^2 copper disk of 1.6 mm thickness and an insulating sensor housing to minimize heat loss from the copper disk. This cylindrical stretching device can be used to replace conventional planar devices in traditional TPP setups to record changes in skin temperature under various fire hazard scenarios (fig. 2).

The heat source consists of two Meker burners and a bank of nine electrically heated quartz tubes that can produce a nominal heat flux of 84 ± 2 kW/m^2 with 50 % radiative and 50 % convective heat. The angle of the Meker burners is kept at 45° to ensure that the flames converge at the center of the specimen. When the burners are turned off, the quartz tubes can be used to simulate low- and medium-intensity radiant heat exposure. The testing specimen remains insulated from the heat source prior to the test through an automatic water-cooled shutter. The temperature increase behind the specimen is measured over time by the cylindrical copper calorimeter. After the heat exposure, the test fabric and copper calorimeter are moved away from the heat source to simulate the cooling process immediately after exposure. The thermal response during this cooling period is also recorded to study the release of thermal energy within protective clothing.

FIG. 2 Schematic of our thermal protective performance tester.

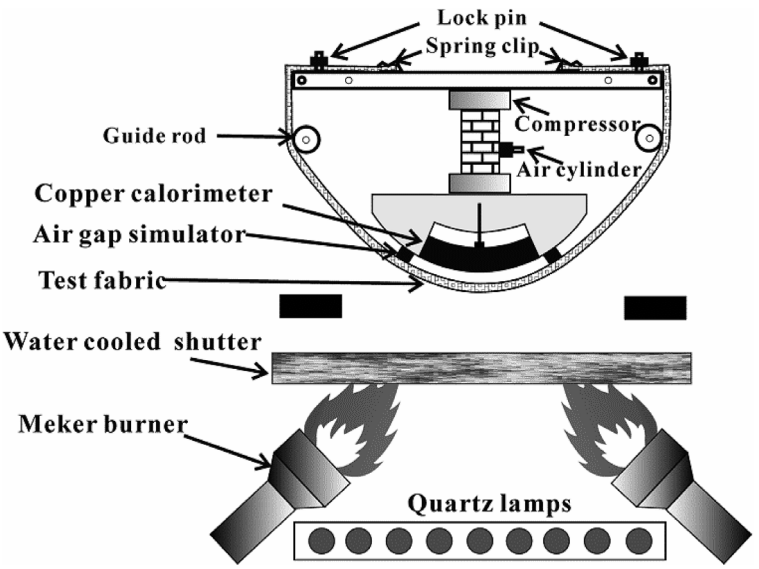

TEST PROCEDURE

Thermal Protective Performance

In accordance with standard ASTM F2703-13, *Standard Test Method for Unsteady-State Heat Transfer Evaluation of Flame Resistant Materials for Clothing with Burn Injury Prediction*,[3] we first calibrated the intensity of the heat source before placing the fabric specimen into the cylindrical sensor assembly and subjecting it to 8.5 kW/m^2 radiative heat and 84 kW/m^2 convective/radiative heat. Prior to heat exposure, we applied one of four different pressures (0, 1.2, 2.1 and 3.1 psi) to stretch the specimen without the presence of any air gap and measured fabric deformation (Table 1). The TPP of the specimen was also evaluated in the presence of a 6.4 mm air gap between the specimen and the copper calorimeter. We exposed the specimen for 120 s to 8.5 kW/m^2 and applied a subsequent cooling period of 120 s. In a second experiment, we exposed the specimen during 10 s to 84 kW/m^2 and applied a subsequent cooling time of 50 s. Controlled heat exposures were started by opening the water-cooled shutter. We then recorded and analyzed the thermal histories behind the fabric system to calculate the times to second- and third-degree skin burn. These values serve as proxies to evaluate the thermal protective capabilities of the fabric system. Each experiment was carried out in triplicate and the final value represents the average.

According to ASTM F2703-13,[3] the measured skin temperatures were used to calculate the incident heat flux to the cooper calorimeter using equation (1):

$$q = \frac{mC_s(T_{i+1} - T_i)}{aA\Delta t} \tag{1}$$

where q is the incident heat flux to the cooper calorimeter, m and C_s are the mass and the average heat capacity of the copper disk, respectively, a is the absorptivity, and A is the area of the exposed copper disk. For predicting deeper skin temperatures and possible burn injuries, the calculated heat flux was treated as the boundary condition in the skin heat transfer model, which takes into account the effect of blood perfusion and metabolic heat on skin heat transition.[25] We assume that skin heat transfer is exclusively one-dimensional and perpendicular to the skin surface. The thermal properties of each layer of skin tissue are assumed constant, while the thermal properties of each layer are different. The blood temperature was assumed to be equal to the core body temperature, and the blood flow rate was assumed to

TABLE 1 Percentage of fabric deformation under different stretching forces

	Percentage of Fabric Deformation (SD)		
Stretching Force (psi)	Fabric A1	Fabric A2	Fabric A3
0	0	0	0
1.2	1.64 % (0.17 %)	4.80 % (0.82 %)	6.00 % (0.26 %)
2.1	11.41 % (0.58 %)	12.65 % (1.07 %)	14.83 % (0.14 %)
3.1	15.05 % (0.18 %)	14.96 % (0.19 %)	15.11 % (0.16 %)

remain constant. The skin heat transfer model in the cylindrical configuration can be expressed as equation (2):[26]

$$(\rho c_p)_{skin}\frac{\partial T}{\partial t} = k_{skin}\left(\frac{\partial^2 T}{\partial r^2} + \frac{1}{r}\frac{\partial T}{\partial r}\right) + w_b(\rho c_p)_b(T_b - T) \quad (2)$$

where ρ_{skin} and $(c_p)_{skin}$ are the density and specific heat of each layer of skin tissue, respectively, ρ_b and $(c_p)_b$ are the density and the specific heat of blood, respectively, w_b is the rate of blood perfusion at the dermis layer and subcutaneous tissue, and T_b is the blood temperature.

Fabric Physical Properties

Applying a stretching force to the fabric changed its physical properties. The thickness of test specimens was measured under a pressure of 5 kPa using a compression tester (KES-FB3-A, Kato Technology Corporation, Japan). The ATLAS air permeability tester was used to measure air permeability of test specimens applying a pressure difference of 0.2 kPa. Different stretching forces were applied to the specimen to keep the same percentage of fabric deformation while measuring air permeability. The mass per unit area was calculated for different stretching forces according to the fabric area and the fabric mass measured by an electronic scale. The area of a fabric can change by applying a stretching force, which in turn affects the mass per unit area. Table 2 lists the basic properties of flame-resistant fabrics under different stretching forces.

STATISTICAL ANALYSIS

The analysis of variance (ANOVA) test for the 8.5 and 84 kW/m^2 heat exposures was carried out using the Statistical Package for Social Science (SPSS) software version 20, including an analysis of the relationship between different stretching forces

TABLE 2 Basic properties of flame-resistant fabrics under different stretching forces

Fabric Code	Fiber Content	Fabric Structure	Stretching Force (Psi)	Thickness (mm)	Air Permeability (dm^3/s)	Mass (g/m^2)
A1	Nomex/ Kevlar	Plain	0	0.93	0.33	248.03
			1.2	0.47	0.37	274.54
			2.1	0.45	0.22	290.52
			3.1	0.44	0.10	298.94
A2	Nomex/ Kevlar/P-140	Twill	0	1.07	0.84	260.07
			1.2	0.59	0.88	291.82
			2.1	0.57	0.69	296.50
			3.1	0.55	0.66	295.78
A3	PBI/Kevlar	Twill	0	0.99	1.13	245.68
			1.2	0.44	0.78	298.97
			2.1	0.41	0.54	314.82
			3.1	0.39	0.34	351.19

and TPP. The paired t-test was used to analyze differences in the time to second-degree skin burn between the two heat exposures. Using a correlation analysis, we investigated the effect of fabric's physical properties (thickness, mass, and air permeability) on the time to second-degree skin burn and the relationship between the time to second-degree skin burn and the amount of thermal energy absorbed by the skin. The significance cutoff was set at $p < 0.05$.

Results and Discussion

EFFECT OF FABRIC DEFORMATION ON SKIN BURN

Figure 3 shows the time to second-degree skin burn with different stretching forces under 8.5 kW/m^2 radiative heat exposure. While all fabrics exhibit reduced protective capabilities with increasing stretching force, the removal of an air gap has the greatest influence on the time to second-degree skin burn. This can be attributed to the fact that air, with its low thermal conductivity, provides a better thermal insulation than commonly used flame-resistant materials.[27] When the fabric is in contact with the skin, increased stretching of the fabric only has minor effects on burn times. While removing air gaps reduces the time to second-degree skin burn by more than 50 %, the detrimental effects due to stretching (in the absence of any air gaps) only range from 8.06 % to 20.16 %.

Increases in the stretching force resulted in higher percentages of fabric deformation (Table 1) and the time to second-degree skin burn is negatively correlated with this percentage of fabric deformation ($r_{A1} = -0.767$, $r_{A2} = -0.873$, $r_{A3} = -0.870$), that is, fabric deformation significantly reduces the time to second-degree skin burn.

FIG. 3 Time to second-degree skin burn under 8.5 kW/m^2 radiative heat exposure (*A*) without and (*B*) with stretching forces. Note the difference in scale.

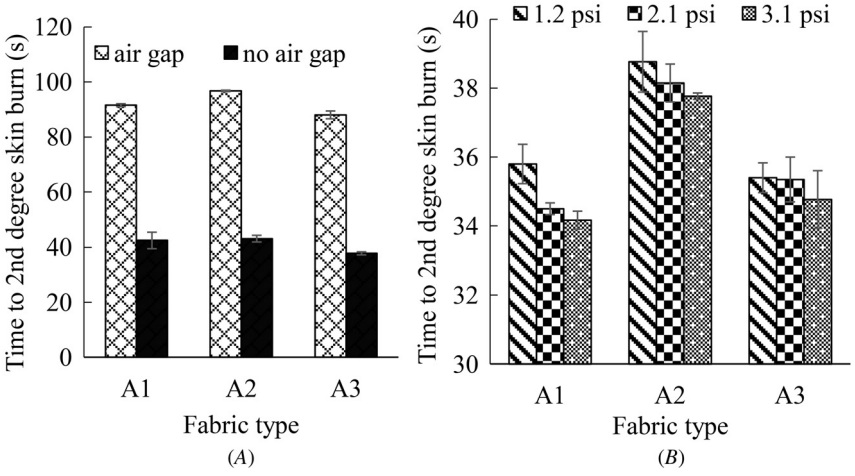

The stretching force also changes the fabric's physical properties (Table 2), such as thickness and air permeability, and increases the mass per unit area of fabric. The fabric's thickness and air permeability were each positively correlated with the time to second-degree skin burn ($r = 0.860$, $p < 0.05$; $r = 0.417$, $p = 0.177$), while we found a negative correlation with the fabric's mass per unit area of fabric ($r = -0.654$, $p < 0.05$). Changes in the physical properties thus affect the conductive and radiative heat transfer in flame-resistant fabrics. The radiative heat transfer in the fabric strongly depends on the transmissivity that is related to the fabric's pore size and ratio.[28] Therefore, decreasing air permeability and increasing the fabric's mass decreases transmissivity and reduces overall radiative heat transfer through the fabric. Conversely, the radiative heat transfer is enhanced by decreasing fabric thickness. The conductive heat transfer in the fabric was determined from the fabric's thickness and thermal conductivity according to Fick's law.[27] Decreasing the fabric's thickness thus increases conductive heat transfer through the fabric. The fabric's thermal conductivity was determined from the fiber to air fraction as shown in equation (3):[28]

$$k_{fab}(T) = V_{air}\%k_{air}(T) + (1 - V_{air}\%)k_{fiber}(T) \tag{3}$$

where $V_{air}\%$ is the percentage of air contained in the fabric's pores, k_{fiber} and k_{air} are the thermal conductivities of fiber and air, respectively (W/m K). As shown in equation (4), $V_{air}\%$ was calculated from the densities of the fabric, ρ_{fab}, the fiber, ρ_{fibre}, and air, ρ_{air}:[28]

$$V_{air}\% = \frac{\rho_{fiber} - \rho_{fab}}{\rho_{fiber} - \rho_{air}} \times 100\,\% \tag{4}$$

The densities of fiber and air are both functions of temperature, while the fabric density is calculated by dividing the mass per area by the fabric's thickness. Therefore, the fabric density changes considerably when stretched. Decreasing $V_{air}\%$ increases the thermal conductivity of fabric, which results in increased conductive heat transfer. Additionally, the transmissivity of commonly used flame-resistant fabrics in most numerical models is around 0.01,[28] indicating that conductive heat transfer dominates in flame-resistant fabrics. Thus, a decrease in fabric thickness and air permeability can reduce TPP, while a decrease of fabric mass has the opposite effect.

The time to second-degree skin burn under 84 kW/m^2 radiative/convective heat exposure (fig. 4) shows a similar trend compared to the 8.5 kW/m^2 scenario ($r = 0.953$, $p < 0.05$) with only minor differences with regard to the effects of stretching forces (summarized in table 3). Compared to the 8.5 kW/m^2 heat exposure, the effect of air gaps is greater in the 84 kW/m^2 heat exposure scenario for fabric A3, but smaller for fabrics A1 and A2. This could be caused by the presence of Nomex fibers in A1 and A2 which can start to degrade at 700 K, thereby causing fabric shrinkage. In addition, the fabric A2, containing flame-resistant cotton, is made by the twill structure, which can further aggravate thermal shrinkage.

FIG. 4 Time to second-degree skin burn under 84 kW/m^2 radiative/convective heat exposure without (*A*) and with (*B*) applied stretching forces.

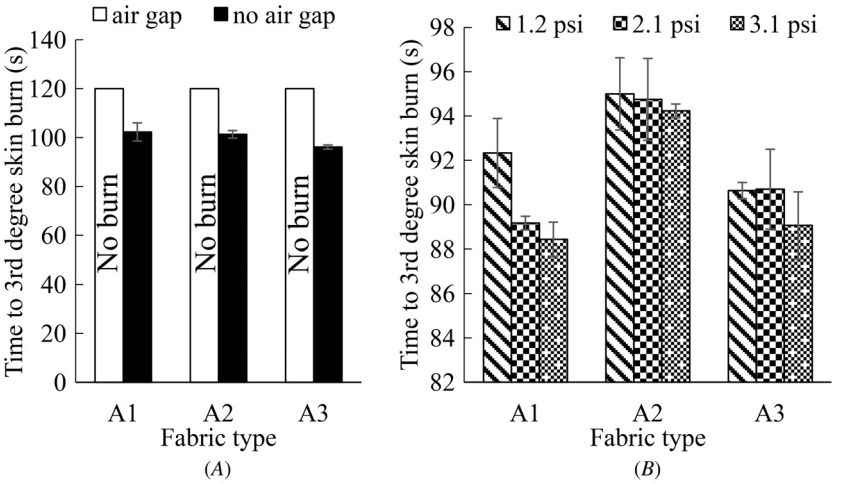

TABLE 3 Differences of second-degree burn time for different heat exposures and stretching forces

	A1		A2		A3	
	8.5 kW/m^2	84 kW/m^2	8.5 kW/m^2	84 kW/m^2	8.5 kW/m^2	84 kW/m^2
Air gap	0	0	0	0	0	0
No air gap (0 psi)	53.68 %	52.49 %	55.55 %	32.19 %	57.08 %	59.91 %
1.2 psi	15.57 %	8.14 %	9.84 %	4.04 %	6.27 %	1.18 %
2.1 psi	3.63 %	2.53 %	1.59 %	5.26 %	0.14 %	1.19 %
3.1 psi	0.97 %	−0.13 %	1.00 %	1.11 %	1.65 %	0.00 %

Note: The differences of second-degree burn time among different stretching forces were calculated from: $Percentage_{0psi} = \frac{T_{Air} - T_{0psi}}{T_{Air}} \times 100\ \%$; $Percentage_{1.2psi} = \frac{T_{0psi} - T_{1.2psi}}{T_{0psi}} \times 100\ \%$; $Percentage_{2.1psi} = \frac{T_{1.2psi} - T_{2.1psi}}{T_{1.2psi}} \times 100\ \%$; $Percentage_{3.1psi} = \frac{T_{2.1psi} - T_{3.1psi}}{T_{2.1psi}} \times 100\ \%$ where *percentage* is the difference of second-degree burn time and T is the second-degree burn time.

This shrinkage leads to greatly reduced air gap sizes with A2, which in turn lowers the fabric's TPP. When applying a stretching force to the 84 kW/m^2 heat exposure scenario, the times until second-degree skin burn are reduced by 2.37 % to 10.41 %, which is less severe than in the 8.5 kW/m^2 radiative heat exposure scenario. Fabric stretching thus has a more pronounced negative impact when the heat exposure is

lower. Theoretically, changes in the fabric's physical properties in response to stretching should be unaffected by heat exposure (i.e., they should be the same before and after the test). However, the higher intensity heat exposure resulted in irreversible thermal degradation that could increase fabric thickness. This was because the thermal degradation formed so-called hornet nest structures.[22]

EFFECT OF FABRIC DEFORMATION ON HEAT FLUX

When comparing the heat flux absorbed by skin under different fabric stretching forces and both heat exposures (**fig. 5**), we found that in the absence of air gaps, increasing stretching forces only produced subtle differences in the observed heat fluxes. The skin heat flux in 8.5 kW/m^2 heat exposure shows a sharp initial increase followed by a slower but steady decrease. For the 84 kW/m^2 heat exposure, the skin heat flux shows a similar sharp initial increase, but the heat flux then remains at this high level or varies slightly depending on the fabric type. The reason for these fabric-dependent differences could lie in the different levels of thermal degradation experienced by each type of fabric under this high-intensity heat exposure.

Once an air gap is introduced, the heat fluxes change considerably both in magnitude and in their course over time. The air gap significantly reduces the heat flux to the skin, indicating that the thermal energy absorbed by the fabric is transferred much faster to the skin if there is no air gap present. This difference is somewhat less pronounced with the fabric A2 which can be attributed to the Nomex and flame-retardant (FR) cotton fibers present in A2 that thermally degrade under the intense 84 kW/m^2 heat exposure, and this is although the fabric A2 has the highest thermal protective level if intact (i.e., nondegraded, cf. the 8.5 kW/m^2 results). In the absence of air gaps, the fabric A2 is capable to maintain its high protective capabilities even in the 84 kW/m^2 exposure scenario. This is because in the absence of air gaps, fabric thickness becomes the key determining factor of TPP.

During the cooling-off period after heat exposure, the presence of air gaps resulted in larger heat fluxes to the skin, indicating a slower heat discharge of the fabric away from the skin. These dynamics largely depend on the discharge of stored thermal energy within the fabric. The existence of an air gap can increase the amount of stored thermal energy within the fabric during heat exposure,[29] thus resulting in a slower discharge of this stored thermal energy once heat exposure has ended. In addition, the existence of air gaps retards heat dissipation from the skin due to the air's insulating thermal properties. The rapid decrease in skin heat flux, even reaching negative values during the cooling period after the 8.5 kW/m^2 heat exposure, indicates the rapid release of thermal energy to the surrounding environment. Applying a stretching force also led to an increase in the discharge rate of skin heat flux as the stretching force reduced fabric thickness and air permeability. During the cooling period that followed the 84 kW/m^2 heat exposure, the skin required more time to reach a negative heat flux due to the larger amount of stored residual heat in the protective clothing.[30] Thus, the discharge of stored thermal energy in the fabric can retard skin cooling.

FIG. 5 Heat flux time series for the 8.5 and 84 kW/m^2 heat exposure scenarios: (*A*) fabric A1 in 8.5 kW/m^2 heat exposure; (*B*) fabric A1 in 84 kW/m^2 heat exposure; (*C*) fabric A2 in 8.5 kW/m^2 heat exposure; (*D*) fabric A2 in 84 kW/m^2 heat exposure; (*E*) fabric A3 in 8.5 kW/m^2 heat exposure; and (*F*) fabric A3 in 84 kW/m^2 heat exposure.

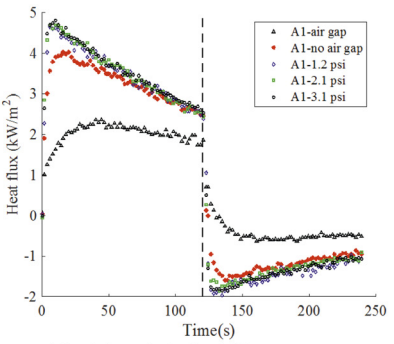

(*A*) Fabric A1 in 8.5 kW/m^2 heat exposure

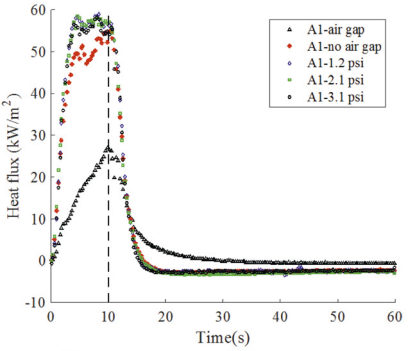

(*B*) Fabric A1 in 84 kW/m^2 heat exposure

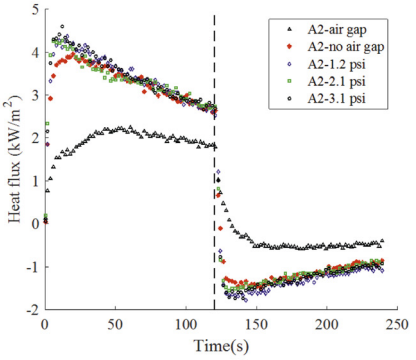

(*C*) Fabric A2 in 8.5 kW/m^2 heat exposure

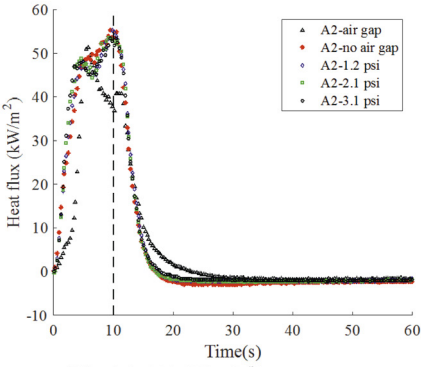

(*D*) Fabric A2 in 84 kW/m^2 heat exposure

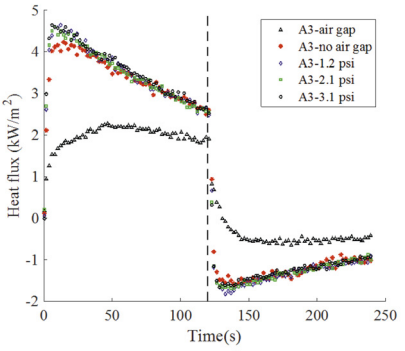

(*E*) Fabric A3 in 8.5 kW/m^2 heat exposure

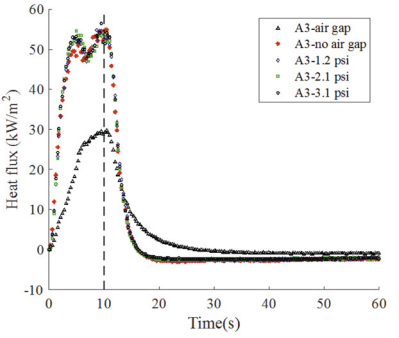

(*F*) Fabric A3 in 84 kW/m^2 heat exposure

Conclusions

We developed a stretching device connected to a cylindrical copper calorimeter to assess the TPP provided by fabrics under realistic conditions of fabric stretching due to movement and changing postures. The stretching-induced changes of the fabric's physical properties were analyzed and the TPP of the fabrics was evaluated. Generally, we found that stretching reduces the protective performance as the applied stretching force negatively affected the fabric's physical properties such as thickness, mass, and porosity. However, under more intense heat exposure, certain fabrics may undergo degradation, which could induce heat release, off-gassing, and shrinkage, and thus lead to more complex changes in its protective properties. Stretching increased the initial heat transfer through the fabric due to the resulting decrease in fabric thickness.

In conclusion, fabric deformations due to body movement and different postures had an important effect on TPP of clothing. Our findings provide some first insight into how to predict the protective performance of personal protective equipment under more realistic conditions and highlight the need to take these factors into account when developing new standardized tests.

ACKNOWLEDGMENTS

This work was sponsored by the Shanghai Sailing Program, National Nature Science Foundation (under Grant No. 51576038), fundamental research funds for the central universities, and initial research funds for young teachers of Donghua University.

References

1. A. H. M. Ali and R. Mohmmed, "A Review of the Firefighting Fabrics for Flashover Temperature," 2015, http://web.archive.org/web/20190405163815/http://citeseerx.ist.psu.edu/viewdoc/summary?doi=10.1.1.695.8267
2. *Standard Test Method for Measuring the Transmitted and Stored Energy of Firefighter Protective Clothing Systems*, ASTM F2731-18 (West Conshohocken, PA: ASTM International, approved June 1, 2018), http://doi.org/10.1520/F2731-18
3. *Standard Test Method for Unsteady-State Heat Transfer Evaluation of Flame Resistant Materials for Clothing with Burn Injury Prediction*, ASTM F2703-08(2013) (West Conshohocken, PA: ASTM International, approved June 1, 2013), http://doi.org/10.1520/F2703-08R13
4. *Standard Test Method for Radiant Heat Performance of Flame Resistant Clothing Materials with Burn Injury Prediction*, ASTM F2702-15 (West Conshohocken, PA: ASTM International, approved February 1, 2015), http://doi.org/10.1520/F2702-15
5. A. M. Stoll and M. A. Chianta, "A Method and Rating System for Evaluation of Thermal Protection," *Aerospace Medicine* 40, no. 11 (1969): 1232–1238.
6. Y. Su, Y. Wang, and J. Li, "Evaluation Method for Thermal Protection of Firefighters' Clothing in High-Temperature and High-Humidity Condition: A Review," *International Journal of Clothing Science and Technology* 28, no. 4 (2016): 429–448.

7. H. H. Pennes, "Analysis of Tissue and Arterial Blood Temperatures in the Resting Human Forearm" *Journal of Applied Physiology* 1, no. 2 (1948): 93–122.
8. F. C. Henriques, Jr., "Studies of Thermal Injury; the Predictability and the Significance of Thermally Induced Rate Processes Leading to Irreversible Epidermal Injury," *Archives of Pathology* 43, no. 5 (1947): 489–502.
9. I. Shalev and R. L. Barker, "Analysis of Heat Transfer Characteristics of Fabrics in an Open Flame Exposure," *Textile Research Journal* 53, no. 8 (1983): 475–482.
10. Y. M. Lee and R. L. Barker, "Thermal Protective Performance of Heat-Resistant Fabrics in Various High Intensity Heat Exposures," *Textile Research Journal* 57, no. 3 (1987): 123–132.
11. R. L. Barker, A. J. Geshury, and W. P. Behnke, "The Effect of Nomex®/Kevlar® Fiber Blend Ratio and Fabric Weight on Fabric Performance in Static and Dynamic TPP Tests," in *Performance of Protective Clothing: Fifth Volume,* ed. J. S. Johnson and S. Z. Mansdorf (West Conshohocken, PA: ASTM International, 1996), 575–591, http://doi.org/10.1520/STP14095S
12. D. A. Torvi and G. V. Hadjisophocleous, "Research in Protective Clothing for Firefighters: State of the Art and Future Directions,"*Fire Technology* 35, no. 2 (1999): 111–130.
13. E. M. Crown, M. Y. Ackerman, J. D. Dale, and Y. B. Tan, "Design and Evaluation of Thermal Protective Flightsuits. Part II: Instrumented Mannequin Evaluation," *Clothing and Textiles Research Journal* 16, no. 2 (1998): 79–87.
14. G. Song, "Clothing Air Gap Layers and Thermal Protective Performance in Single Layer Garment," *Journal of Industrial Textiles* 36, no. 3 (2007): 193–205.
15. T. Mah and G. W. Song, "Investigation of the Contribution of Garment Design to Thermal Protection. Part 1: Characterizing Air Gaps Using Three-dimensional Body Scanning for Women's Protective Clothing," *Textile Research Journal* 80, no. 13 (2010): 1317–1329.
16. H. Mäkinen, J. Smolander, and H. Vuorinen, "Simulation of the Effect of Moisture Content in Underwear and on the Skin Surface on Steam Burns of Fire Fighters," in *Performance of Protective Clothing: Second Symposium*, ed. S. Mansdorf, R. Sager, and A. Neilsen (West Conshohocken, PA: ASTM International, 1988), 415–421, http://doi.org/10.1520/STP26309S
17. M. Fu, W. G. Weng, and H. Y. Yuan, "Quantitative Assessment of the Relationship between Radiant Heat Exposure and Protective Performance of Multilayer Thermal Protective Clothing during Dry and Wet Conditions," *Journal of Hazardous Materials* 276 (2014): 383–392.
18. L. Xin, X. Li, and J. Li, "A New Approach to Evaluate the Effect of Body Motion on Heat Transfer of Thermal Protective Clothing during Flash Fire Exposure," *Fibers and Polymers* 15, no. 10 (2014): 2225–2231.
19. A. Ghazy and D. J. Bergstrom, "Numerical Simulation of the Influence of Fabric's Motion on Protective Clothing Performance during Flash Fire Exposure," *Heat and Mass Transfer* 49, no. 6 (2013): 775–788.
20. P. Talukdar, A. Das, and R. Alagirusamy, "Numerical Modeling of Heat Transfer and Fluid Motion in Air Gap between Clothing and Human Body: Effect of Air Gap Orientation and Body Movement,"*International Journal of Heat and Mass Transfer* 108 (2017): 271–291.
21. J. Li, X. Li, Y. Lu, and Y. Wang, "A New Approach to Characterize the Effect of Fabric Deformation on Thermal Protective Performance," *Measurement Science and Technology* 23, 4 (2012): 045601.
22. Y. Su, R. Li, J. Yang, G. Song, and J. Li, "Developing a Test Device to Analyze Heat Transfer through Firefighter Protective Clothing," *International Journal of Thermal Sciences* 138 (2019): 1–11.

23. Z. Cui and W. Zhang, "Study of the Effect of Material Assembly on the Moisture and Thermal Protective Performance of Firefighter Clothing," *Fibres & Textiles in Eastern Europe* 17, no. 6 (2009): 80–83.
24. F. Zhu and K. Li, "Numerical Modeling of Heat and Moisture through Wet Cotton Fabric Using the Method of Chemical Thermodynamic Law under Simulated Fire," *Fire Technology* 47, no. 3 (2011): 801–819.
25. D. A. Torvi and J. D. Dale, "A Finite Element Model of Skin Subjected to a Flash Fire," *Journal of Biomechanical Engineering* 116, no. 3 (1994): 250–255.
26. D. A. Hodson, G. Eason, and J. C. Barbenel, "Modeling Transient Heat Transfer through the Skin and Superficial Tissues—1: Surface Insulation," *Journal of Biomechanical Engineering* 108, no. 2 (1986): 183–188.
27. J. P. Holman, "Heat Transfer,"*McGraw-Hill Higher Education* 46, no. 3 (2011): 121–130.
28. D. A. Torvi, "Heat Transfer in Thin Fibrous Materials under High Heat Flux Conditions" (PhD diss., University of Alberta, 1997).
29. Y. Su, J. He, and J. Li, "Modeling the Transmitted and Stored Energy in Multilayer Protective Clothing under Low-Level Radiant Exposure," *Applied Thermal Engineering* 93 (2016): 1295–1303.
30. G. Song, F. Gholamreza, and W. Cao, "Analyzing Thermal Stored Energy and Effect on Protective Performance," *Textile Research Journal* 81, no. 11 (2011): 1124–1138.